

of the *hgcAB* cluster in the genomes of several sequenced, but so far untested, microorganisms (table S4) leads us to hypothesize that these organisms are also capable of methylating mercury. The gene cluster appears to be quite sporadically distributed across two phyla of bacteria (Proteobacteria and Firmicutes) and one phylum of archaea (Euryarchaeota). Organisms possessing the two-gene cluster include 24 strains of Deltaproteobacteria, 16 Clostridia, 1 Negativicutes, and 11 Methanomicrobia. Interestingly, we also found these genes in a psychrophile (30), in a thermophile (31), and in a human commensal methanogen (32) (Fig. 3). The sparse phylogenetic gene distribution of the *hgcAB* system may be due to gene loss or lateral gene transfer (or both) across distant taxa and may be linked to environmental and community-structure factors. The sporadic distribution of these genes and the lack of an obvious selective advantage related to mercury toxicity (15) raise important questions regarding their physiological roles. Identification of these genes is a critical step linking specific microorganisms and environmental factors that influence microbial Hg methylation in aquatic ecosystems.

References and Notes

1. J. M. Wood, *Science* **183**, 1049 (1974).
2. H. Hintelmann, *Met. Ions Life Sci.* **7**, 365 (2010).
3. G. C. Compeau, R. Bartha, *Appl. Environ. Microbiol.* **50**, 498 (1985).
4. C. C. Gilmour, E. A. Henry, R. Mitchell, *Environ. Sci. Technol.* **26**, 2281 (1992).

5. E. J. Fleming, E. E. Mack, P. G. Green, D. C. Nelson, *Appl. Environ. Microbiol.* **72**, 457 (2006).
6. E. J. Kerin *et al.*, *Appl. Environ. Microbiol.* **72**, 7919 (2006).
7. R. Q. Yu *et al.*, *Environ. Sci. Technol.* **46**, 2684 (2012).
8. J. M. Wood, F. S. Kennedy, C. G. Rosen, *Nature* **220**, 173 (1968).
9. S. Hamelin, M. Amyot, T. Barkay, Y. P. Wang, D. Planas, *Environ. Sci. Technol.* **45**, 7693 (2011).
10. J. K. Schaefer *et al.*, *Proc. Natl. Acad. Sci. U.S.A.* **108**, 8714 (2011).
11. S. C. Choi, T. Chase Jr., R. Bartha, *Appl. Environ. Microbiol.* **60**, 4072 (1994).
12. S. C. Choi, T. Chase Jr., R. Bartha, *Appl. Environ. Microbiol.* **60**, 1342 (1994).
13. E. B. Ekstrom, F. M. Morel, J. M. Benoit, *Appl. Environ. Microbiol.* **69**, 5414 (2003).
14. M. Ranchou-Peyruse *et al.*, *Geomicrobiol. J.* **26**, 1 (2009).
15. C. C. Gilmour *et al.*, *Appl. Environ. Microbiol.* **77**, 3938 (2011).
16. R.-Q. Yu *et al.*, *Environ. Sci. Technol.* **46**, 2684 (2012).
17. T. I. Doukov, T. M. Iverson, J. Seravalli, S. W. Ragsdale, C. L. Drennan, *Science* **298**, 567 (2002).
18. Y. Kung *et al.*, *Nature* **484**, 265 (2012).
19. S. W. Ragsdale, P. A. Lindahl, E. Münck, *J. Biol. Chem.* **262**, 14289 (1987).
20. T. Svetlitchnaia, V. Svetlitchnyi, O. Meyer, H. Dobbek, *Proc. Natl. Acad. Sci. U.S.A.* **103**, 14331 (2006).
21. S. Goetzl, J. H. Jeoung, S. E. Hennig, H. Dobbek, *J. Mol. Biol.* **411**, 96 (2011).
22. S. D. Brown *et al.*, *J. Bacteriol.* **193**, 2078 (2011).
23. M. Punta *et al.*, *Nucleic Acids Res.* **40** (database issue), D290 (2012).
24. H. L. Drake, S. I. Hu, H. G. Wood, *J. Biol. Chem.* **256**, 11137 (1981).
25. T. Doukov, J. Seravalli, J. J. Stezowski, S. W. Ragsdale, *Structure* **8**, 817 (2000).
26. P. Cardiano, G. Falcone, C. Foti, S. Sammartano, *J. Chem. Eng. Data* **56**, 4741 (2011).

27. R. E. DeSimone *et al.*, *Biochim. Biophys. Acta* **304**, 851 (1973).
28. H. A. O. Hill, J. M. Pratt, S. Ridsdale, F. R. Williams, *J. Chem. Soc. Chem. Commun.* **1970**, 341 (1970).
29. G. N. Schrauzer, J. W. Sibert, *J. Am. Chem. Soc.* **92**, 3509 (1970).
30. G. S. Zhang, N. Jiang, X. L. Liu, X. Z. Dong, *Appl. Environ. Microbiol.* **74**, 6114 (2008).
31. G. B. Slobodkina *et al.*, *Int. J. Syst. Evol. Microbiol.* **62**, 2463 (2012).
32. B. Dridi, M. L. Fardeau, B. Ollivier, D. Raoult, M. Drancourt, *Int. J. Syst. Evol. Microbiol.* **62**, 1902 (2012).

Acknowledgments: We thank S. Miller, C. Gilmour, and T. Barkay for helpful discussions, and K. Rush, X. Yin, G. Christensen, and Q. Gui for experimental assistance. Supported by the U.S. Department of Energy (DOE), Office of Science, Office of Biological and Environmental Research, through the Mercury Scientific Focus Area Program at Oak Ridge National Laboratory (ORNL). ORNL is managed by UT Battelle, LLC, for DOE under contract DE-AC05-00OR22725. All other data are available online in the supplementary materials. Author contributions: J.M.P., A.J., R.B., J.C.S., A.V.P., D.A.E., S.D.B., M.P., J.D.W., and L.L. designed the research. M.P., S.D.B., and C.C.B. performed the comparative genomic analyses. A.J. and J.M.P. performed the bioinformatics and biochemical interpretations. R.B., R.A.H., S.D.S., S.J.T., A.J., and Y.Q. performed the experiments. J.M.P., A.J., R.B., J.C.S., D.A.E., J.D.W., and L.L. wrote the paper.

Supplementary Materials

www.sciencemag.org/cgi/content/full/science.1230667/DC1
Materials and Methods
Supplementary Text
Figs. S1 to S9
Tables S1 to S8
References (33–69)

24 September 2012; accepted 23 January 2013
Published online 7 February 2013;
10.1126/science.1230667

The *C9orf72* GGGGCC Repeat Is Translated into Aggregating Dipeptide-Repeat Proteins in FTL/ALS

Kohji Mori,^{1*} Shih-Ming Weng,^{2*} Thomas Arzberger,³ Stephanie May,² Kristin Rentzsch,² Elisabeth Kremmer,⁴ Bettina Schmid,^{2,5} Hans A. Kretzschmar,³ Marc Cruts,^{6,7} Christine Van Broeckhoven,^{6,7} Christian Haass,^{1,2,5} Dieter Edbauer^{1,2,5†}

Expansion of a GGGGCC hexanucleotide repeat upstream of the *C9orf72* coding region is the most common cause of familial frontotemporal lobar degeneration and amyotrophic lateral sclerosis (FTLD/ALS), but the pathomechanisms involved are unknown. As in other FTLD/ALS variants, characteristic intracellular inclusions of misfolded proteins define *C9orf72* pathology, but the core proteins of the majority of inclusions are still unknown. Here, we found that most of these characteristic inclusions contain poly-(Gly-Ala) and, to a lesser extent, poly-(Gly-Pro) and poly-(Gly-Arg) dipeptide-repeat proteins presumably generated by non-ATG-initiated translation from the expanded GGGGCC repeat in three reading frames. These findings directly link the FTLD/ALS-associated genetic mutation to the predominant pathology in patients with *C9orf72* hexanucleotide expansion.

Frontotemporal lobar degeneration (FTLD) and amyotrophic lateral sclerosis (ALS) are the extreme ends of a spectrum of overlapping neurodegenerative disorders variably associated with dementia, personality changes, language abnormalities, and progressive muscle

weakness (1–3). The majority of patients show intracellular inclusions that are strongly positive for phosphorylated TDP-43 (classified as FTLD-TDP, FTLD/ALS-TDP, or ALS-TDP). Recently, expansion of a GGGGCC hexanucleotide repeat in the gene *C9orf72* has been identified as the

most common pathogenic mutation in families with autosomal dominant FTLD, FTLD/ALS, and ALS (4–6). The expansion is located upstream of the *C9orf72* coding region, either in the first intron or the promoter region, depending on the transcript isoform (fig. S1A). Although the extreme GC content precludes sequencing in patients, the number of GGGGCC repeat units is believed to be at least several hundred, compared with fewer than 25 in healthy controls (7).

Patients with a *C9orf72* repeat expansion mutation have clinical symptoms similar to other FTLD/ALS-TDP patients but show several unique

¹Adolf Butenandt-Institute, Biochemistry, Ludwig-Maximilians University (LMU) Munich, Schillerstrasse 44, 80336 Munich, Germany. ²German Center for Neurodegenerative Diseases (DZNE), Munich, Schillerstrasse 44, 80336 Munich, Germany. ³Center for Neuropathology and Prion Research, Ludwig-Maximilians-University Munich, Feodor-Lynen-Strasse 23, 81377 Munich, Germany. ⁴Institute of Molecular Immunology, Helmholtz Zentrum München, Marchioninistrasse 25, 81377 Munich, Germany. ⁵Munich Cluster of Systems Neurology (SyNergy), Ludwig-Maximilians-University Munich, Schillerstrasse 44, 80336 Munich, Germany. ⁶Neurodegenerative Brain Diseases Group, Department of Molecular Genetics, VIB, Universiteitsplein 1, B-2610 Antwerp, Belgium. ⁷Laboratory of Neurogenetics, Institute Born-Bunge, University of Antwerp, Universiteitsplein 1, B-2610 Antwerp, Belgium.

*These authors contributed equally to this work.

†To whom correspondence should be addressed. E-mail: dieter.edbauer@dzne.de

pathological features (8–12). Aggregates of phosphorylated TDP-43 are accompanied by abundant dotlike and star-shaped phospho-TDP-43–negative neuronal cytoplasmic inclusions—in particular, in cerebellum, hippocampus, and frontotemporal neocortex—that can only be identified with antibodies for p62, ubiquitin, or the related ubiquilins (8–11). These phospho-TDP-43–negative aggregates are highly characteristic of diseased *C9orf72* mutation carriers and are absent in other variants of FTL/ALS-TDP (9–11). The identity of the disease protein(s) in these inclusions and their relation to the *C9orf72* hexanucleotide repeat expansion have remained elusive. Proposed pathomechanisms include haploinsufficiency through impaired transcription or splicing of the mutant *C9orf72* allele and RNA toxicity through the sequestration of unidentified RNA-binding proteins (3–7).

We hypothesized that the intronic GGGGCC repeat might be aberrantly translated into dipeptide-repeat (DPR) proteins. Although quite rare, two mechanisms of non-ATG–initiated translation have been described: Initiation from alternative start codons with a good Kozak sequence is possible (13–15), and hairpin formation in the repeat region may trigger so-called repeat-associated non-ATG–initiated (RAN) translation, as described for CAG repeats in ataxin 8 (*ATXN8*) (16–18). *ATXN8* encodes a natural poly-Q stretch that can cause poly-Q inclusions upon repeat expansion in spinocerebellar ataxia type 8 (SCA8) patients. Strikingly, the expanded CAG repeat is translated in all three reading frames (poly-Q, poly-A, and poly-S) even after removal of the endogenous start codon.

Translation of the GGGGCC repeat in all reading frames would result in three DPR proteins: poly-(Gly-Ala), poly-(Gly-Pro), and poly-(Gly-Arg). poly-GA and poly-GP proteins are extremely hydrophobic and may form intracellular aggregates. We raised antibodies (anti-GA and anti-GP) against (GA)₁₅ and (GP)₁₅ peptides fused to maltose binding protein and tested a monoclonal antibody (anti-GR) that was originally raised against an EBNA2A epitope with a (GR)₆ repeat (19). All three affinity-purified DPR antibodies detected the respective repeat antigen by immunoblotting without cross-reaction with the other two DPR proteins (Fig. 1A).

To investigate whether such repeat proteins can be translated in the absence of a start codon, we cloned parts of the repeat region from *C9orf72* patients into a mammalian expression vector. For the longer constructs, we could only use restriction digest to estimate the repeat number ranging from ~28 to ~145 (Fig. 1B), because the extreme GC content precludes sequencing. The region upstream of the GGGGCC repeat lacks ATG start codons and contains four to five stop codons, depending on the reading frame. Upon transfection of these constructs into human embryonic kidney (HEK) 293 cells, anti-GA detected proteins of increasing size starting with a faint product from ~38 repeats, suggesting that the translation

mechanism becomes more efficient with increasing repeat length (Fig. 1B). We did not detect poly-GR products, and only the longest construct with ~145 repeats additionally expressed detectable amounts of poly-GP (Fig. 1B).

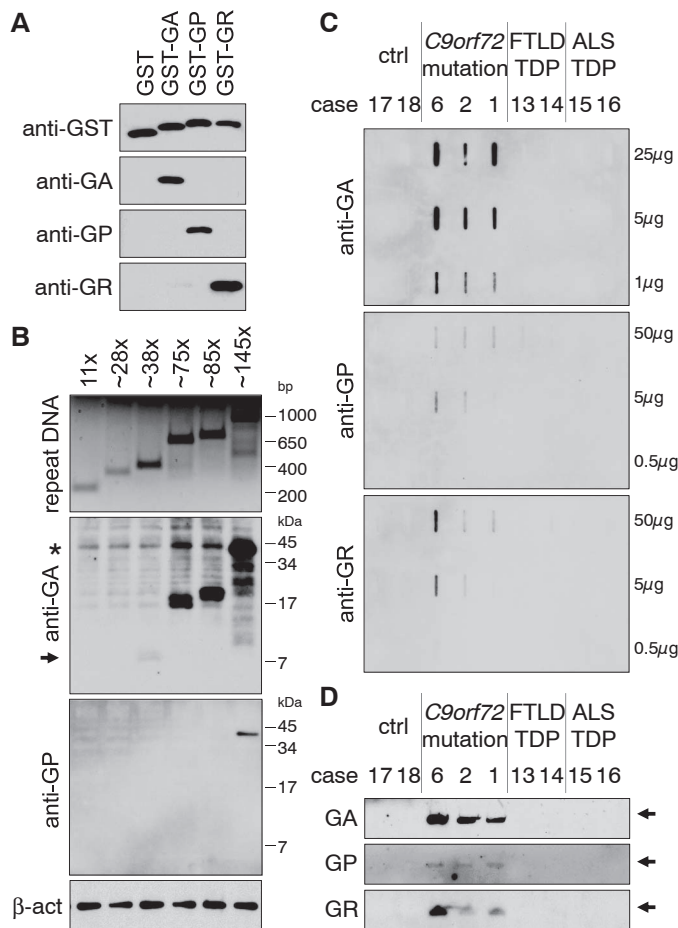
To analyze poly-GA aggregation, we performed filter trap assays (20) using 2% sodium dodecyl sulfate (SDS) extracts from human postmortem cerebellum of healthy controls and FTL/ALS-TDP patients with and without pathological *C9orf72* hexanucleotide repeat expansion. We observed strong poly-GA signal only in FTL/ALS patient with hexanucleotide repeat expansion (Fig. 1C), indicating that poly-GA forms SDS-insoluble aggregates in the cerebellum. We also detected insoluble poly-GP and poly-GR in *C9orf72* patients (Fig. 1C). The 2% SDS-insoluble material was partially solubilized upon boiling in 8% SDS and could be analyzed by immunoblotting. We detected high-molecular weight DPR aggregates in all three reading frames at the top of the gel specifically in patients with *C9orf72* mutation (Fig. 1D).

mRNA expression of the mutant *C9orf72* allele is reported to be repressed through impaired transcription or splicing (4, 6, 7). We also found

reduced *C9orf72* mRNA levels in patient cerebellum (fig. S1B). However, both sense and antisense transcripts containing intron 1 (where the GGGGCC repeat is located) were strongly increased in *C9orf72* patients (fig. S1C). This suggests a selective stabilization of repeat containing pre-mRNA (or the excised intron 1 alone) and raises the possibility that the antisense strand may be translated into poly-(Pro-Arg), poly-(Ala-Pro) and further poly-GP DPR proteins.

To determine the cellular distribution patterns of these DPR proteins in patients with pathological *C9orf72* repeat expansion, we focused on the cerebellum and hippocampus in the immunohistochemical analysis because these brain regions contain abundant inclusion pathology positive for p62 but negative for phospho-TDP-43 (9–11) (Fig. 2, A and B, and fig. S2A). In all patients with *C9orf72* mutation, poly-GA–specific antibodies detected dotlike neuronal cytoplasmic inclusions in the granular cell layer of the cerebellum (Fig. 2C and fig. S2B). Their shape and abundance were similar to the p62-positive/TDP-43–negative inclusions considered to be pathognomonic for *C9orf72* mutation patients.

Fig. 1. Extended GGGGCC repeats are translated into aggregating DPR proteins. (A) Validation of DPR-specific affinity-purified antibodies by immunoblotting with purified GST-fusion proteins containing (GA)₁₅, (GP)₁₅, or (GR)₁₅. **(B)** GGGGCC-repeat constructs with indicated repeat length lacking an upstream ATG were transfected into HEK293 cells. Restriction digest to estimate the repeat length of the transfected constructs (upper panel). Immunoblots show length-dependent expression of poly-GA and poly-GP proteins. Poly-GA products were detectable starting from ~38 repeats (arrow). Asterisk indicates nonspecific band. Poly-GR products were not detected (not shown). **(C)** Filter trap assay from patient cerebellum (table S1). Triton-X100 insoluble fractions were re-suspended in 2% SDS and filtered through cellulose acetate membranes, and retained proteins were detected with the indicated antibodies. **(D)** The SDS-insoluble fraction from (C) was boiled in 4x Laemmli buffer (containing 8% SDS) and analyzed by immunoblotting. Arrows mark the top of the gel. Single-letter abbreviations for the amino acid residues are as follows: A, Ala; C, Cys; D, Asp; E, Glu; F, Phe; G, Gly; H, His; I, Ile; K, Lys; L, Leu; M, Met; N, Asn; P, Pro; Q, Gln; R, Arg; S, Ser; T, Thr; V, Val; W, Trp; and Y, Tyr.



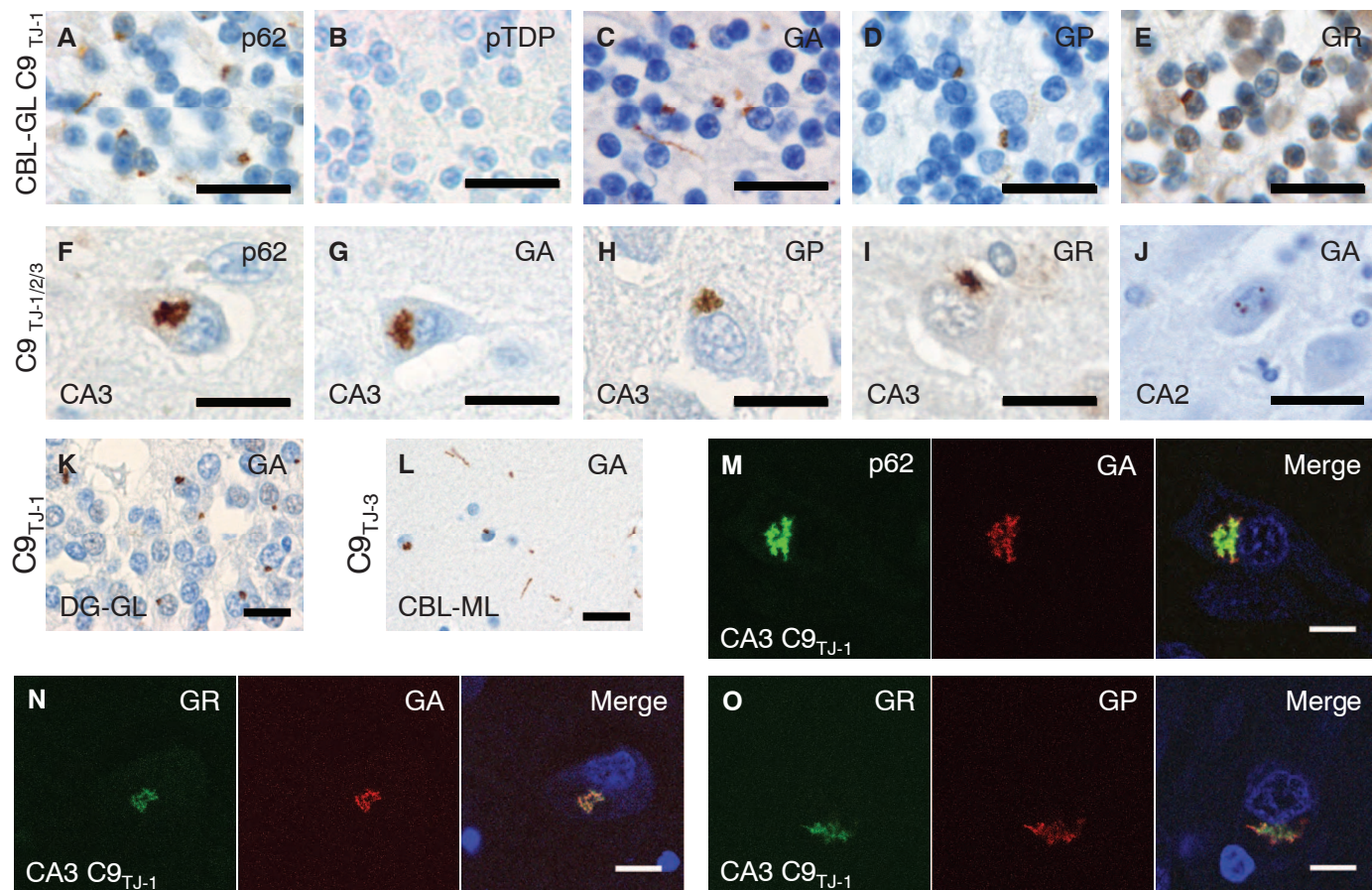
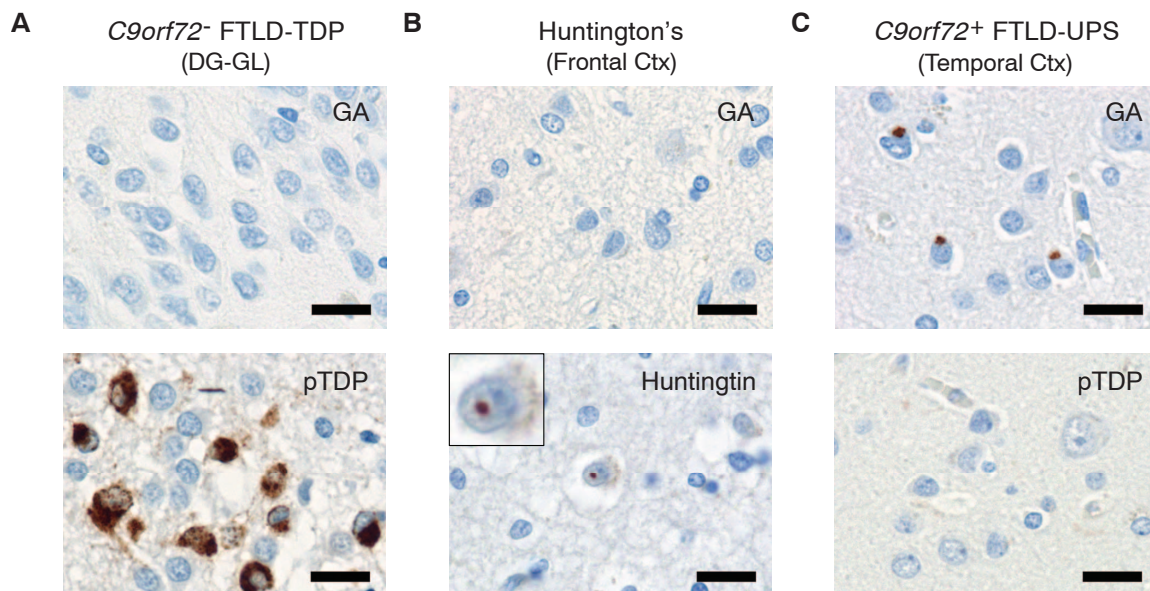


Fig. 2. DPR proteins form the characteristic TDP-43-negative inclusions in *C9orf72* patients. Immunohistochemistry with affinity-purified DPR-specific antibodies (GA, GP, and GR) reveals poly-GA, poly-GP, and poly-GR inclusions resembling the p62-positive aggregates in FTLD/ALS patients with *C9orf72* mutation (compare table S1). Dotlike and threadlike inclusions in cerebellar granular layer (CBL-GL) (A to E). Star-shaped cytoplasmic (F to I) and dot-like intranuclear (J) inclusions in hippocampal cornu ammonis regions 2 and 3 (CA2 and CA3). Inclusion of mixed morphology in dentate gyrus granular layer (DG-GL) and cerebellar molecular layer (CBL-ML) (K and

L). In patients and controls, poly-GR antibodies additionally showed faint nuclear and cytoplasmic staining. Scale bars, 20 μ m. Anti-GA and anti-GP specificity was confirmed by preincubation experiments with recombinant antigens (fig. S3, A to F). Validation of anti-GR was only possible by immunoblot experiments (Fig. 1A) because the poly-GR antigen itself bound to the tissue directly (fig. S3, G to K). (M to O) Double immunofluorescence reveals composition of DPR aggregates in *C9orf72* FTLD/ALS patient TJ-1. No colocalization of DPR proteins was observed with phospho-TDP-43 (fig. S4). Scale bars, 10 μ m.

Fig. 3. DPR pathology is specific to patients with *C9orf72* hexanucleotide repeat expansion. (A and B) Immunohistochemistry with poly-GA-specific antibodies (GA) detects no aggregates in an FTLD-TDP patient (TJ-13) without *C9orf72* repeat expansion and a case with Huntington's disease (TJ-11). Phospho-TDP-43 and Huntingtin inclusions are readily detectable. Granular layer of dentate gyrus (DG-GL) and frontal cortex, respectively. (C) Poly-GA-positive inclusions, but no phospho-TDP-43 inclusions, in temporal cortex of patient TJ-10 with *C9orf72* mutation diagnosed with FTLD-UPS (6). Scale bars, 20 μ m.



Furthermore, these types of inclusions were also detected by antibodies against poly-GP and poly-GR, however to a much lesser extent (Fig. 2, D and E, and fig. S2, C and D). In the hippocampus, most inclusions stained by the three DPR antibodies resembled the p62-positive star-shaped inclusions typical for *C9orf72* mutation patients (Fig. 2, F to I, and fig. S3). As reported for p62 stainings (9, 11), we also observed some DPR-positive neuronal intranuclear inclusions (Fig. 2J). Their relation to the RNA foci described previously remains to be determined (4). Similar DPR pathology was visible in other brain regions, including the granular layer of the dentate gyrus and the molecular layer of the cerebellum and neocortex (Fig. 2, K and L, and table S1).

We next analyzed whether the DPR-positive aggregates are identical to the p62-positive and phospho-TDP-43-negative aggregates. In hippocampal sections of a *C9orf72* mutation patient, poly-GA, poly-GP, and poly-GR colocalized with p62 in the characteristic starlike inclusions (Fig. 2, M to O, and fig. S4, D and E). However, there was no coaggregation of phospho-TDP-43 and DPR proteins (fig. S4, A to C). Occasionally, small spheric poly-GA aggregates were surrounded by aggregated phospho-TDP-43, forming a core inside phospho-TDP-43 inclusions (fig. S4F), which suggests that DPR aggregation may precede TDP-43 pathology. Quantitative analysis confirmed extensive colocalization of p62-positive inclusions with poly-GA aggregates and, to a lesser extent, with poly-GP and poly-GR (fig. S4G).

Consistent with the filter trap assay (Fig. 1C), such poly-GA aggregates were not detectable in FTLT-DTP patients without *C9orf72* mutation or with Huntington's disease, which features expanded poly-Q stretches (Fig. 3, A and B). In total, we identified poly-GA, poly-GP, and poly-GR aggregates in all 10 patients with a confirmed pathological *C9orf72* repeat expansion but not in 12 other cases with normal repeat length (table S1).

Some patients with *C9orf72* mutation show remarkably few phospho-TDP-43 inclusions throughout the brain. So far, only a single exceptional patient (TJ-10)—classified as FTLT-UPS (ubiquitin pro-

teasome system), with *C9orf72* mutation and prominent ubiquitin-pathology but without detectable TDP-43 pathology—has been reported (6, 7). We found abundant poly-GA and some poly-GP and poly-GR aggregates in the temporal cortex of this patient (Fig. 3C and table S1), suggesting that DPR proteins are crucial for FTLT pathogenesis in this case. Thus, we propose that poly-GA is the main aggregating species in FTLT-UPS patients with *C9orf72* repeat expansion.

Here, we have shown that non-ATG-initiated translation of the intronic GGGGCC-repeat expansion in FTLT/ALS patients leads to accumulation of insoluble DPR aggregates. In addition to DPR and TDP-43 pathology, the *C9orf72* expansion may lead to haploinsufficiency and trigger sequestration of GGGGCC-binding proteins. Such interacting proteins may even support nuclear export of the repeat RNA or its translation.

Ample evidence suggests a pathogenic role of DPR inclusions in FTLT patients with *C9orf72* hexanucleotide repeat expansion. First, DPR pathology is predominant in clinically relevant brain regions (hippocampus and frontotemporal neocortex) and may precede TDP-43 pathology. Second, *C9orf72* patients show cerebellar atrophy that does not occur in the other FTLT/ALS variants lacking cerebellar DPR inclusions (10, 12). Third, at least one *C9orf72* mutation carrier had abundant DPR pathology and behavioral-variant clinical FTLT but no detectable TDP-43 inclusion pathology. Finally, DPR pathology is a direct consequence of the pathological hexanucleotide repeat expansion, the most common genetic cause of FTLT/ALS. We therefore suggest the acronym FTLT/ALS-DPR to pathologically classify these patients in a revised nomenclature.

References and Notes

1. K. A. Josephs *et al.*, *Acta Neuropathol.* **122**, 137 (2011).
2. I. R. Mackenzie, R. Rademakers, M. Neumann, *Lancet Neurol.* **9**, 995 (2010).
3. R. Rademakers, M. Neumann, I. R. Mackenzie, *Nat. Rev. Neurol.* **8**, 423 (2012).
4. M. DeJesus-Hernandez *et al.*, *Neuron* **72**, 245 (2011).
5. A. E. Renton *et al.*, *Neuron* **72**, 257 (2011).
6. I. Gijssels *et al.*, *Lancet Neurol.* **11**, 54 (2012).
7. J. van der Zee *et al.*, *Hum. Mutat.* **34**, 363 (2013).
8. A. L. Boxer *et al.*, *J. Neurol. Neurosurg. Psychiatry* **82**, 196 (2011).

9. S. Al-Sarraj *et al.*, *Acta Neuropathol.* **122**, 691 (2011).
10. C. J. Mahoney *et al.*, *Brain* **135**, 736 (2012).
11. E. H. Bigio *et al.*, *Neuropathology* (2012); 10.1111/j.1440-1789.2012.01332.x.
12. J. L. Whitwell *et al.*, *Brain* **135**, 794 (2012).
13. I. P. Ivanov, A. E. Firth, A. M. Michel, J. F. Atkins, P. V. Baranov, *Nucleic Acids Res.* **39**, 4220 (2011).
14. D. S. Peabody, *J. Biol. Chem.* **264**, 5031 (1989).
15. C. Touriol *et al.*, *Biol. Cell* **95**, 169 (2003).
16. T. Zu *et al.*, *Proc. Natl. Acad. Sci. U.S.A.* **108**, 260 (2011).
17. C. E. Pearson, *PLoS Genet.* **7**, e1002018 (2011).
18. M. L. Moseley *et al.*, *Nat. Genet.* **38**, 758 (2006).
19. E. Kremmer *et al.*, *Virology* **208**, 336 (1995).
20. H. Li, T. Wyman, Z. X. Yu, S. H. Li, X. J. Li, *Hum. Mol. Genet.* **12**, 2021 (2003).

Acknowledgments: We thank I. Pigur for technical assistance, M. Neumann for genotyping of some of the LMU cases, and J. Banzhaf-Strathmann, F. van Bebber, E. Bentmann, D. Dormann, J. Herms, A. Hruscha, G. Kleinberger, J. McCarter, D. Orozco, and B. Schwenk for critical comments. This project was supported by a grant from the Centres of Excellence in Neurodegeneration Research (CoEN) to M.C., C.H., C.V.B., B.S., and D.E., and the Competence Network for Neurodegenerative Diseases (KNDD) of the Bundesministerium für Bildung und Forschung (BMBF) to C.H. K.M. was supported by a postdoctoral fellowship from the Alexander von Humboldt Foundation. D.E. was supported by the Helmholtz Young Investigator program. We thank all clinicians recruiting brain donors, in particular H.-H. Klünemann (Bezirksklinikum Regensburg) and, most notably, all brain donors and their next of kin. We acknowledge the Antwerp biobank of the Institute Born-Bunge for brain samples, as well as T. Van Langenhove, J. van der Zee, S. Engelborghs, P. P. De Deyn, A. Sieben, and J.-J. Martin for genetic, clinical, and pathological diagnoses. The Antwerp site is supported by the MetLife Foundation Award (to C.V.B.), the Belgian Science Policy Office Interuniversity Attraction Poles program, the Foundation for Alzheimer Research (SAO/FRA), the Medical Foundation Queen Elisabeth, the Flemish Government Methusalem excellence program, the Research Foundation Flanders (FWO), and the University Research Fund of the University of Antwerp. A patent application concerning DPR-based diagnosis and therapy of neurodegenerative disorders has been filed by K.M., S.-M.W., T.A., K.R., E.K., C.H., and D.E.

Supplementary Materials

www.sciencemag.org/cgi/content/full/science.1232927/DC1
Materials and Methods
Supplementary Text
Figs. S1 to S4
Table S1
References (21, 22)

19 November 2012; accepted 25 January 2013
Updated online 7 February 2013;
10.1126/science.1232927

This copy is for your personal, non-commercial use only.

If you wish to distribute this article to others, you can order high-quality copies for your colleagues, clients, or customers by [clicking here](#).

Permission to republish or repurpose articles or portions of articles can be obtained by following the guidelines [here](#).

The following resources related to this article are available online at www.sciencemag.org (this information is current as of February 27, 2015):

Updated information and services, including high-resolution figures, can be found in the online version of this article at:

<http://www.sciencemag.org/content/339/6125/1335.full.html>

Supporting Online Material can be found at:

<http://www.sciencemag.org/content/suppl/2013/02/06/science.1232927.DC1.html>

A list of selected additional articles on the Science Web sites **related to this article** can be found at:

<http://www.sciencemag.org/content/339/6125/1335.full.html#related>

This article **cites 22 articles**, 7 of which can be accessed free:

<http://www.sciencemag.org/content/339/6125/1335.full.html#ref-list-1>

This article has been **cited by** 45 articles hosted by HighWire Press; see:

<http://www.sciencemag.org/content/339/6125/1335.full.html#related-urls>

This article appears in the following **subject collections**:

Neuroscience

<http://www.sciencemag.org/cgi/collection/neuroscience>